https://doi.org/10.5194/egusphere-2025-8
Preprint. Discussion started: 3 March 2025

Unprecedent cave ice melt in the last 6100 years in the Central Pyrenees (A294 ice cave)

Carlos Sancho[1†], Ánchel Belmonte[2], Maria Leunda[3,4,5], Marc Luetscher[6], Christoph Spötl[7], Juan Ignacio López-Moreno[8], Belén Oliva-Urcia[1], Jerónimo López-Martínez[9], Ana Moreno[8], Miguel Bartolomé*[6, 10, 11]

1 Departamento de Ciencias de la Tierra, Universidad de Zaragoza, C/ Pedro Cerbuna, 12, 50009 Zaragoza, Spain

2 Sobrarbe-Pirineos UNESCO Global Geopark, Avda. Ordesa 79, 22340 Boltaña, Spain

3 Department of Plant Biology and Ecology, Faculty of Science and Technology, University of the Basque Country (UPV-EHU), Barrio Sarriena s/n, 48940, Leioa, Bizkaia, Spain

4 Swiss Federal Institute for Forest, Snow and Landscape Research WSL Zürcherstrasse 111, 8903 Birmensdorf, Switzerland

5 Institute of Plant Sciences & Oeschger Centre for Climate Change Research University of Bern, Alternbergrain 21, 3012, Bern, Switzerland

6 Swiss Institute for Speleology and Karst Studies (SISKA), Rue de la Serre 68, 2300 La Chaux-de-Fonds, Switzerland

7 Institute of Geology, University of Innsbruck, Innrain 52, 6020 Innsbruck, Austria

8 Departamento de Procesos Geoambientales y Cambio Global, Instituto Pirenaico de Ecología (CSIC), Avda. Montañana 1005, 50059 Zaragoza, Spain

9 Facultad de Ciencias, Universidad Autónoma de Madrid, Francisco Tomás y Valiente 7, 28049 Madrid, Spain

10 Geological Institute, NO G59, Department of Earth Sciences, Sonneggstrasse 5, ETH, 8092 Zurich, Switzerland

11 Departamento de Geología, Museo Nacional de Ciencias Naturales (CSIC), C/ de José Gutiérrez Abascal, 2, 28006 Madrid, Spain

† Deceased

*Correspondence to: mbart@mncn.csic.es

https://doi.org/10.5194/egusphere-2025-8
Preprint. Discussion started: 3 March 2025

ABSTRACT

Ice caves are understudied environments within the cryosphere, hosting unique ice deposits valuable for paleoclimate studies. Recently, many of these deposits have experienced accelerated retreat due to global warming, threatening their existence. The A294 cave contains the world's known oldest firn cave deposit (6100 years cal. BP), which is progressively waning. This study presents 12 years (2009-2021) of monitoring data from A294, including temperature measurements both outside and inside the cave, meteoric precipitation, and ice loss measurements by comparing historical cave surveys (1978, 2012, 2019), photographs, and ice measurements within the cave. Our findings indicate a continuous increase in cave air temperature (~1.07 to 1.56 °C over 12 years), increases in the Thaw Index, and a decrease in the number of freezing days (i.e., days below 0 °C) as well as in the Freezing Index. Calculated melting rates based on cave surveys and measurements show significant variations depending on the cave sector, ranging from ~15 to ~192 cm per year. The retreat of the ice body is primarily driven by an increase in winter temperatures, the rise in rainfall during the warm seasons, and the decrease in snowfall and snow cover duration. The ice stratigraphy and local paleoclimate records suggest unprecedented melting conditions since this ice began to form 6100 years ago. This study highlights the urgent need to recover all possible information from these unique subterranean ice deposits before they disappear.

1. Introduction

The mean global temperature has risen by 0.8 to 1.1 °C since the early 20th century (IPCC, 2021). However, specific mountainous regions in Southern Europe, such as the Pyrenees, have experienced a temperature surge of ~1.3 °C since 1949 (Observatorio Pirenaico de Cambio Global, 2018), indicating an acceleration in warming nearly twice as much as the global average. This temperature increase is directly impacting the glaciers in the Pyrenees, which have receded significantly since the end of the Little Ice Age (González Trueba et al., 2008; García-Ruiz et al.,

https://doi.org/10.5194/egusphere-2025-8
Preprint. Discussion started: 3 March 2025

2014). The pace of this retreat has notably accelerated in recent years (López-Moreno et al., 2016; Vidaller et al., 2021, 2023). Glaciers are not the only elements of the cryosphere affected by global warming: Mountain permafrost and ice caves are also facing critical threats (Kern and Perşoiu, 2013; Biskaborn et al., 2019), with ice caves representing the least studied systems.

The scientific community has recognized the pressing need for a comprehensive research initiative aimed at recovering untapped physical, chemical, and biological information stored within cave ice bodies prior to their complete disappearance (Kern and Perşoiu, 2013). Unlike glaciers, mid-latitude ice caves are less vulnerable to summer temperature fluctuations and thus have the potential to preserve paleoclimate data over longer periods. Ice caves have therefore attracted a great deal of attention for research into this unique repository of past climatic conditions (Luetscher et al., 2005; Stoffel et al., 2009; Feurdean et al., 2011; Žák et al., 2012; Perșoiu et al., 2017; Sancho et al., 2018; Leunda et al., 2019; Racine et al., 2022a; Racine et al., 2022b; Bartolomé et al., 2023; Ruiz-Blas et al., 2023).

In static ice caves (i.e. sag-type), the ingress of cold and dense air during the winter season cools the ice cave (open phase), while during the warm season, the cave operates as a cold trap (closed phase), with the influence of higher temperatures being nearly negligible (Luetscher et al., 2008). The ice retreat within these ice caves is predominantly regulated by diminished winter precipitation and rising winter temperatures (Luetscher et al., 2005, 2008). The heat exchanged during winter determines the cave temperatures during the closed phase thereby affecting ice melting (Wind et al., 2022). Additionally, the increase in rainfall and extreme precipitation events during warmer seasons (closed phase in ice caves) leads to ice loss due to the release of heat through the penetration of water into the cave environment (Luetscher et al., 2008; Perşoiu et al., 2021). Monitoring the current cave dynamics helps to understand how caves work and thus to recognize the factors that influence the melting of cave ice (Luetscher et al., 2008; Perşoiu et al., 2021; Wind et al., 2022; Bartolomé et al., 2023).

https://doi.org/10.5194/egusphere-2025-8
Preprint. Discussion started: 3 March 2025

In this study, we present a comprehensive dataset derived from a 12-year monitoring campaign (2009-2021) in A294 ice cave, situated in the Central Pyrenees. The rise in cave temperature and the increase in summer and fall precipitation pose a significant threat to the oldest documented firn in the world, which is preserved in a cave and is between 6100 and 1880 years old (Sancho et al., 2018). The data we have gathered and the analysis of ice stratigraphy and climate reconstructions since the onset of the Neoglacial period provide compelling evidence that the ongoing melting of this exceptional ice body represents the most significant retreat since its accumulation began 6100 years ago.

2. The A294 ice cave

This ice cave is located in the Central Pyrenees (Belmonte-Ribas et al., 2014), in the north-eastern part of the Iberian Peninsula (Fig. 1a). The cave is situated in the Cotiella massif, at an elevation of 2238 m a.s.l. This massif belongs to the Central South Pyrenean Unit and it consists mainly of Upper Cretaceous limestones as well as Eocene limestones and marls (Supplementary material, Fig. S1). The highest point in this area is the Cotiella peak at 2912 m a.s.l. (Fig. 1b). The Armeña cirque is characterized by periglacial and karst landforms (Fig. 1b). In this region, there is a climatic transition between the Atlantic and Mediterranean mountain climates. The mean annual air temperature (MAAT) at the nearby Armeña Weather Station (AWS, Fig. 1b, c, d) at 2200 m a.s.l. elevation averages ~5.6 ºC (2009-2021; Fig. 1c). The wettest periods in this area are in April/May and October/November. Winters and summers are typified by cold and warm/dry periods, respectively (Fig. 1c). During the colder months, there are more than 20 snowfalls a year between November and April. In the Central Pyrenees, at 2000 m a.s.l. the average snow depth typically ranges between 20 and 80 cm (1985-1999) with annual peaks that often exceed 150 cm. Superimposed on a very large interannual variability, the duration of the snow cover and the accumulation of snow depth have decreased statistically significant since the middle of the 20th century (López-Moreno, 2005; López-Moreno et al., 2020). At higher altitudes, around 2600 m a.s.l., the snow depth at the end of winter is often more than 3 m (López-Moreno et al., 2019).

https://doi.org/10.5194/egusphere-2025-8
Preprint. Discussion started: 3 March 2025

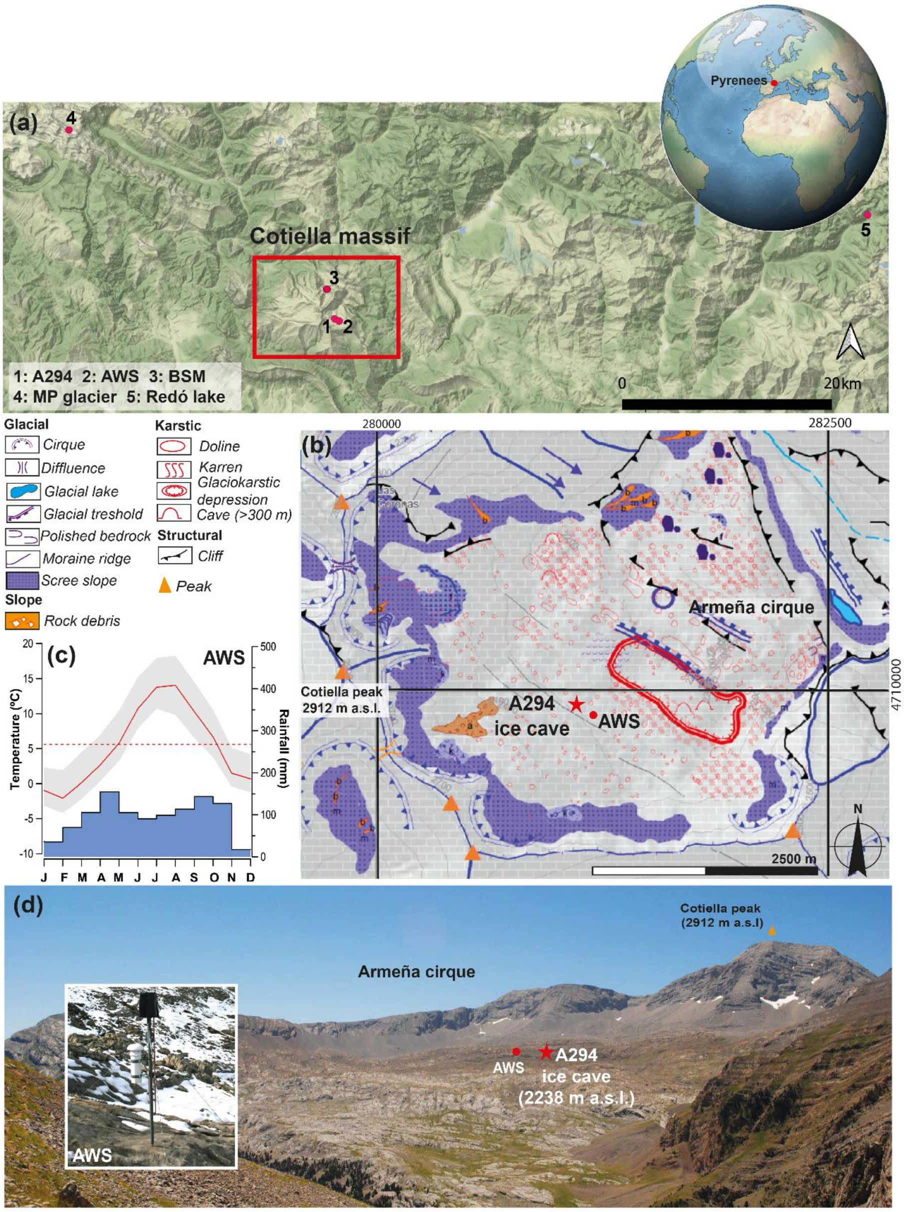

Figure 1. a) Location of the Cotiella massif in the Central Pyrenees and the different paleoclimate records and the weather station used in this study (1: A294 ice cave (A294), 2: Armeña Weather Station (AWS), 3: Basa de la Mora (lake, BSM), 4: Monte Perdido glacier (MP glacier), 5: Redó lake). b) Geomorphological map and location of the A294 ice cave and the weather station (modified from Belmonte, 2014). c)

https://doi.org/10.5194/egusphere-2025-8
Preprint. Discussion started: 3 March 2025

Monthly mean temperature (red line), maximum and minimum mean temperatures (grey shaded area), annual mean temperature (dashed red line) and mean monthly rainfall (blue bars) over the last 12 years recorded at the Armeña Weather Station (AWS) located at 2200 m a.s.l., ~400 m east of the A294 cave entrance (d).

The A294 cave is a sag-type cave, with a depth of ~40 m and two entrances (Fig. 2a, b). The primary entrance consists of a vertical shaft that is ~10 m high and spans an area of roughly 30 m^2. There is also a second, smaller shaft that is typically closed off by snow in the winter months. The primary entrance is connected via a snow ramp to the cave main chamber, which contains an old ice body (Fig. 2a). The thickness and extent of the snow ramp varies from year to year, depending on the frequency and intensity of snowfall (Belmonte-Ribas et al., 2014). Open conditions marked by a chimney effect characterize the winter phase (November–May). Ventilation occurs primarily via the main shaft, while the smaller shaft is usually blocked by snow during fall, winter and sometimes in spring. Conversely, cave acts as a cold air trap during the closed phase (June–October) (Fig. 2b). Two areas in the cave host seasonal ice stalagmites (IS 1 and 2) underneath several active dripping points (Fig. 2a).

https://doi.org/10.5194/egusphere-2025-8
Preprint. Discussion started: 3 March 2025

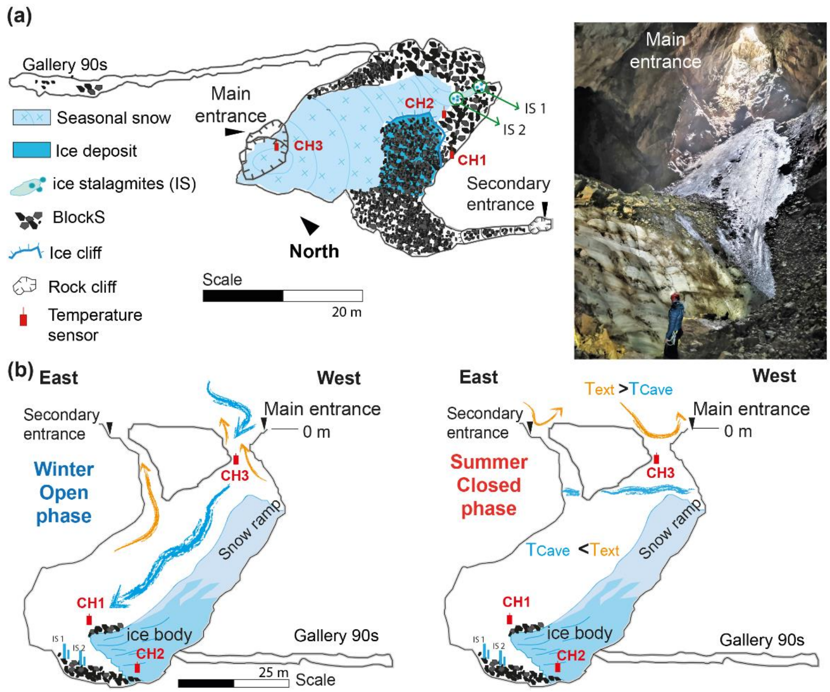

Figure 2: a) Geomorphological map superimposed on the 2019 cave survey. The location of temperature sensors is indicated in red. The light blue colour represents seasonal snow and the dark blue colour represents the fossil ice body. IS1 and IS2 indicate seasonal ice stalagmites. b) Cave profile with a simplified model of air circulation during winter (open phase, left) and summer (closed phase, right). Blue arrows show the movement of cold air masses, while orange arrows represent warm air fluxes inside the cave. Photo: David Serrano.

3. Material and methods

3.1 Ice extent

The ice retreat was assessed on the basis of cave surveys from different years (1978, 2012, 2019, Fig. 3a, b, c, d). The surveys of 1978 (Grupo de Espeleología Cataluña Aragón, G.E.C.A.) and 2012 (Belmonte-Ribas et al., 2014) were carried out with a normal compass and clinometer. The North arrow in the original 1978 survey was not correctly positioned, and the crevasse between ice and bedrock is questionable, as in 2008 the old ice on the southern wall was in contact with the bedrock (Fig. S2).

https://doi.org/10.5194/egusphere-2025-8
Preprint. Discussion started: 3 March 2025

The crevasse must have been small, because the new gallery (Gallery 90s) was found during the 90s when the ice had retreated far enough (Fig. 2). The survey in 2019 (Fig. 2) was conducted using a DistoX2 Leica (X310) modified with an electronic base plate to measure the direction and dip (Heeb, 2014). A total of 68 points were measured emphasizing cave morphology and the ice perimeter. To determine the horizontal retreat of the ice body, the ice perimeter was determined at three reference points/sectors defined in Fig. 3 (number 1 to 3). To evaluate vertical changes of the ice body during the monitored period, two stratigraphic logs were made (Sancho et al., 2018; Leunda et al., 2019) (Fig. S3). In 2011, when the deposit was first sampled, the ice was 9.25 m thick and decreased to 7.90 m in 2015 when the second stratigraphic log was prepared. The internal structure of the ice sequence also changed between 2011 and 2015 (Leunda et al., 2019) as shown by the cross-stratified ice beds formed during snow deposition. Nevertheless, the identification of a same detrital layer (observed at 165 cm depth from the top in 2015 and at 240 cm depth in 2011) allows comparing the depth-age models for both years (Fig. S3). The spatio-temporal reproducibility of the depth-age models together with the good correspondence between two independently dated terrestrial plant macrofossil remains reveals that, although decadal-scale melting periods may have occurred repeatedly, the macrofossil remains preserved in the detrital layers did not suffer significant movements within the ice deposit. Complementary field measurements using fixed reference points (blocks, walls, dripping points) together with several photographs taken between 2008 and 2023 were also used to reconstruct the changes in size of the ice body.

https://doi.org/10.5194/egusphere-2025-8
Preprint. Discussion started: 3 March 2025

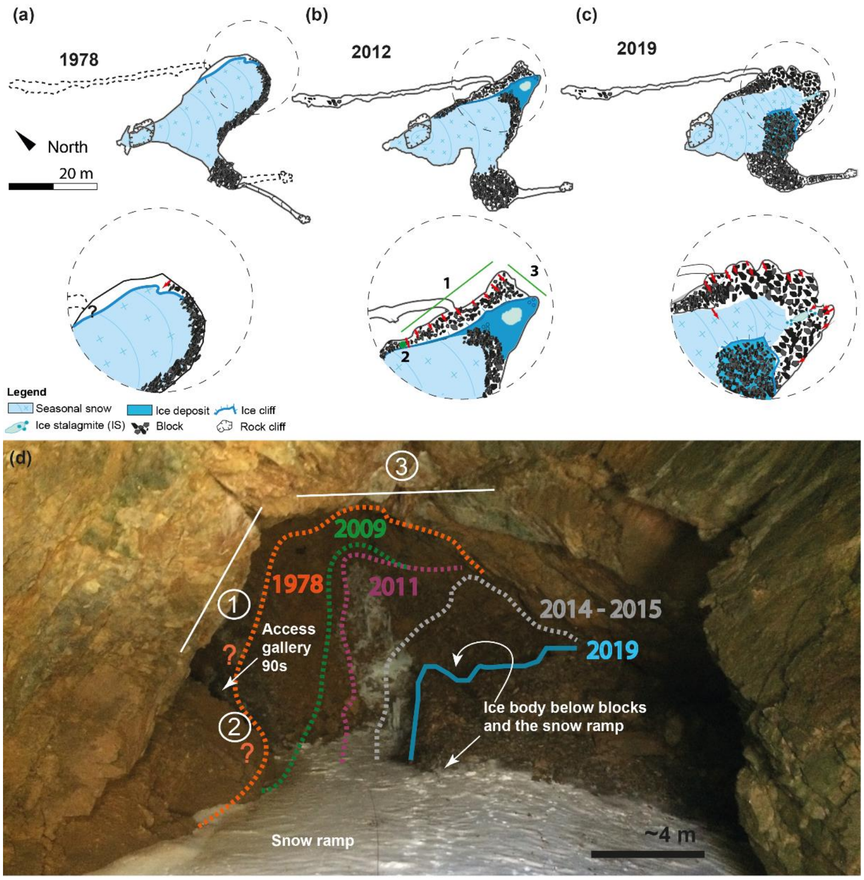

Figure 3: Three plan view maps of the A294 ice cave from different surveys. a) Corrected cave topography from 1978 ((G.E.C.A), see Fig. S2 for details). *Note: The dashed galleries on the 1978 survey indicate a cave passage discovered in 2012 and the corrected position of the southern gallery, respectively. b) Cave survey from 2012 (Belmonte et al., 2014). c) Cave survey from 2019 (this study). The insets, marked with black dashed circles, correspond to sectors where topographic changes were measured and indicated by numbers: (1) Northern wall, (2) Rock corner (green point) and (3) Ice front. Red arrows correspond to distances selected for measurements on the cave surveys, and some of them in the field. d) Photograph taken from the main shaft, showing the approximate position of the ice body between 1978 and 2019.

167

https://doi.org/10.5194/egusphere-2025-8
Preprint. Discussion started: 3 March 2025

3.2 Environmental monitoring

The cave air temperature was recorded over 12 years (2009-2021) (Fig. 4) using Hobo Pro v2 U23-001 sensors with an accuracy of ±0.21 ºC and a resolution of 0.02 ºC at 0 ºC. In 2009, six sensors were installed in the cave, of which the three time series with the longest and most complete temperature records (CH1, CH2 and CH3) were used for this study (same labels as in Belmonte-Ribas et al., 2014). The sensors were set up with a 1-hour logging interval, from which the mean, maximum (max) and minimum (min) daily temperatures were calculated. The Freezing index (FI), defined as the integral of the temperatures below freezing during a given freezing season (approximately mid-October to April) (Tuhkanen, 1980) was calculated for each station. Similarly, the Thaw Index, (TI), was calculated for positive temperatures (Harris, 1981). To characterize (Fig. 4) the thermal regime of the cave, the temperatures were divided into different groups and the respective percentages (%) per month were calculated. These groups include positive temperatures, and temperatures ranging from <0 to -2 ºC, <-2 to -3 ºC, <-3 to -4 ºC, and < -4 ºC. The thermal open phases begin on the first day (dd/mm/aa), when negative cave temperatures are recorded in the cave (even if they briefly become positive again), while their end corresponds to the last day with negative temperatures inside. The closed phase is delimited by two open phases, when the cave temperature is constantly positive. Once the open and closed phase (dd/mm/yy) have been defined, the same periods were selected for outside temperature correlations. Correlations between the different parameters were calculated using the PAST software (Hammer et al., 2001).

The Armeña Weather Station (AWS) was installed in 2011 and the air temperature is measured with an EL-USB-1 instrument with an accuracy of ±0.5 ºC and a resolution of 0.5 ºC. A radiation shield was installed to protect the sensor. The temperature gaps from 2009 to 2011 were filled using the two closest meteorological records available above 2000 m a.s.l., the Góriz and La Renclusa stations, located 28 and 30 km from the cave respectively. Given the difficulty of finding highly significant correlations between meteorological records located in an area with complex

https://doi.org/10.5194/egusphere-2025-8
Preprint. Discussion started: 3 March 2025

topography (Beguería et al., 2019), we used a quantile-based approach (Lompar et al., 2019) to reconstruct a the temperature series. Accordingly, all temperature data were transformed to quantiles, based on their empirical cumulative distribution function. The gaps in the timeseries were filled using the quantile values of the Góriz station, and in case data were also missing at this site (less than 1% of the records), we used the ones from La Renclusa. We tested this procedure using the period 2014-2016 as validation, and we obtained 0.13 ºC and 0.55 ºC of Mean Bias Error (MBE) and Mean Absolute Error (MAE), respectively. Snow accumulation was recorded at the Góriz station. To register rainfall events, a pluviometer was installed and connected to a Hobo event (Pendant UA-003-64). Only liquid precipitation was recorded between April to November.

3.3 Radiocarbon dating

Terrestrial plant remains were retrieved from two pit holes formed in the ice ramp in 2022. The samples were analysed at Direct AMS (Seattle, USA) and were calibrated using the Clam 2.2 package (Blaauw, 2010) and R (R Core Team, 2020) and using the INTCAL 20 calibration curve (Reimer et al., 2020).

https://doi.org/10.5194/egusphere-2025-8
Preprint. Discussion started: 3 March 2025

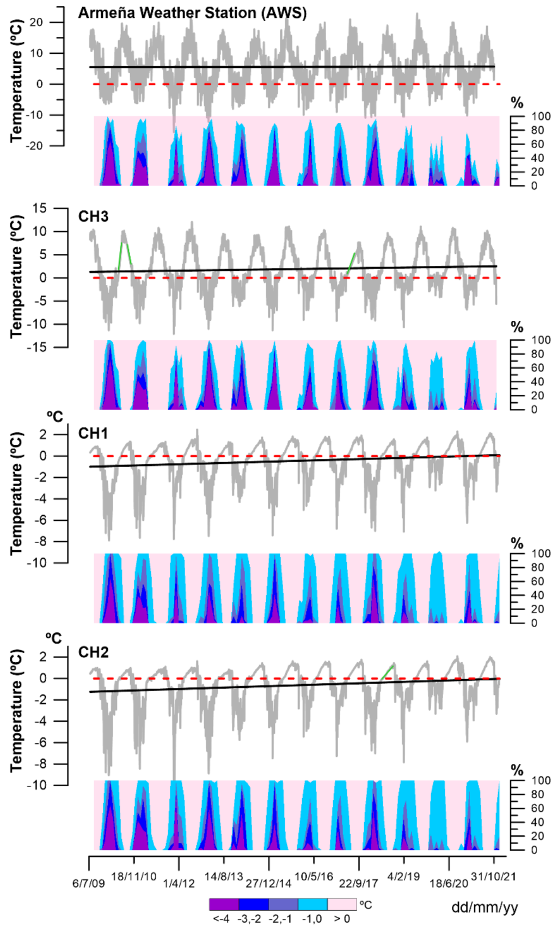

Figure 4: 12 years of cave and Armeña Weather Station (AWS) temperature and characterization of the thermal state based on five temperature clusters. The dashed red line marks 0 ºC; the black line represents the temperature trend. Note that the green lines correspond to reconstructed datasets.

4. Results

a. The old ice body

The ice body in the A294 cave primarily originates from snow that has fallen or slid into the cave (Belmonte-Ribas et al., 2014; Sancho et al., 2018; Leunda et al., 2019). This deposit is characterized by the presence of cross-stratified ice and detrital layers formed by clasts and terrestrial plant macro-remains (Sancho et al., 2018). Notably, there are no indications of congelation ice in this succession. The deposit

https://doi.org/10.5194/egusphere-2025-8
Preprint. Discussion started: 3 March 2025

studied in 2011 and 2015 (Sancho et al., 2018; Leunda et al., 2019) comprised five units separated by ice unconformities (Fig. 5a, b, c). These unconformities were created by sedimentary contacts parallel to the ice beds (paraconformities) and erosional contacts that cut across underlying beds (disconformities). Detrital layers correspond to decadal-scale ablation periods (Sancho et al., 2018). However, three of these unconformities represent longer periods with low snow and ice accumulation between ~5515-4945, ~4250-3810, and ~3155-2450 years ago, indicating rather extended periods when the ice accumulation ceased, potentially due to drier and relatively warmer winters (Sancho et al., 2018). The ice accumulation ended about 1890 years ago (Sancho et al., 2018).

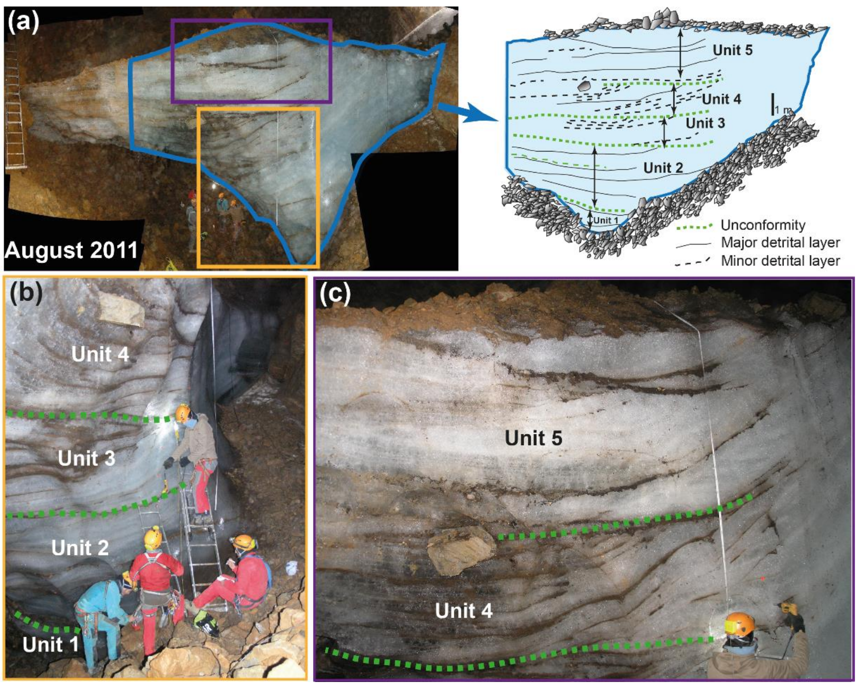

Figure 5. a) Panoramic picture of the cliff of the A294 ice body showing its internal structure as identified by Sancho et al. (2018). b) and c) detail of ice stratigraphy including unconformities recognized in 2011 (Sancho et al., 2018).

In 2022, for the first time in 13 years of observation, the snow on the ramp disappeared completely at the beginning of fall allowing to sample directly the ice

https://doi.org/10.5194/egusphere-2025-8
Preprint. Discussion started: 3 March 2025

underneath the annual snow layer. At the base of the ramp, the ice layers follow the ramp's slope and become more horizontal towards the top of the deposit. Two ablation pits (Fig. 6) formed by drips during the exceptionally warm summer of 2022 (Serrano-Notivoli et al., 2023) allowed the recovery of plant macro remains. The first sample from the middle part of the ramp provided a ^{14}C age ranging from 1509 to 1310 cal. yr BP (A294 R-mid, mean age 1409±99 (614±99 Common Era, CE)). The second sample, retrieved from about 1.5 m below the top of the deposit (approximately 15 m above the main ice body), ranges between 906 and 736 cal. yr BP (A294 R-top; mean 821±85, (1202±85 CE)) (Fig. 6 and Table S1).

Lab. code	**Sample name**	**Material**	**Radiocarbon age (^{14}C year BP)**	**Radiocarbon age 2σ (cal. yr BP)**
D-AMS 049893	A294 R-top	Terrestrial plant remains	908±24	736-906
D-AMS 049894	A294 R-mid	Terrestrial plant remains	1510±30	1310-1509

Table 1: Radiocarbon dates of terrestrial plant macrofossils of the A294 ice cave sampled in December 2022.

Figure 6. Ablation pit located close to the top of the ramp, horizontal detrital-rich ice layers, location of sample A294 R-Top and its age. Photo taken on 27th December 2022. Note that the fresh snow dates from the fall, while in October 2022 the ramp was snow-free (Fig. S3).

https://doi.org/10.5194/egusphere-2025-8
Preprint. Discussion started: 3 March 2025

Abundant blocks cover the ice body at the base of the ramp, forming a protalus rampart (Belmonte-Ribas et al., 2014), reaching a thickness of 50-60 cm (Fig. 1d). This accumulation implies that the upper section of the ice body has remained relatively stable for an extended period. The earliest cave survey from 1978 indicated that the ice body was in contact with the entire cave perimeter, except for a small ablation pit hole and a narrow rimaye (Fig. S2). The current shape of the ice body in the lower part is characterized by an overhanging part, while the ice surface displays scallops ranging from decimeters to meters in scale (Fig. 2).

4.2 Climate and cave environment variability over the last 12 years

Analysis of the temperature data from the Armeña Weather Station (AWS) depicts notable trends over the past 12 years. The mean winter temperature (WT) (Fig. 7a) shows a warming trend, with an increase of 0.07 °C a^{-1} on average, resulting in a cumulative rise of 0.86 °C over the study period. Concurrently, the number of freezing days during winter exhibits a slight decrease at a rate of approximately 1 day a^{-1} (Fig. 7b). The Freezing Index (FI) and the Thaw Index (TI) (Fig. 7c) reveal an increase and a marginal decrease, respectively.

In the A294 cave, sensors CH1 and CH2 are positioned at the top (around -23 m) and bottom (approximately -33 m) of the ice body, respectively, while CH3 is located near the cave entrance (at roughly -6 m). Over the 12-year period, the mean temperature displays negative values at CH1 (-0.45 °C) and CH2 (-0.64 °C), whereas CH3 recorded a positive mean value (+1.91 °C). The mean annual cave air temperature increased significantly at all sensors over the 12 years (Fig. 2): CH1 increased by 0.08 °C a^{-1}, totalling 1.07 °C; CH2 increased by 0.10 °C a^{-1}, totalling 1.28 °C; CH3 increased by 0.13 °C a^{-1}, summing up to 1.56 °C. The number of freezing days (Fig. 2b) decreased at CH1 (3.3 days a^{-1}, 40 days in total), CH3 (1.3 days a^{-1}, 16 days in total), an in CH2 (0.44 days a^{-1}, 5.3 days in total). The record reveals a decreasing number of freezing days for all calculated temperature ranges (Fig. 4).

https://doi.org/10.5194/egusphere-2025-8
Preprint. Discussion started: 3 March 2025

The data from the AWS highlights a slight increase (decrease) in the FI and TI, respectively (Fig. 2c). Inside the cave, the CH2 and CH3 sensors exhibit the lowest mean FI values (-370 and -339 °C hours per year, respectively), whereas CH1 show a slightly higher mean value (-333 °C hours per year), which maybe is related to the position of the sensor close to the ice deposit. In contrast, CH2 and CH3 are more exposed to cold temperatures given their position. The TI shows slightly higher values at CH1 compared to CH2 (158 vs. 122 °C hours per year), while CH3 presents the highest values (962 °C hours per year), evidently influenced by the external temperature.

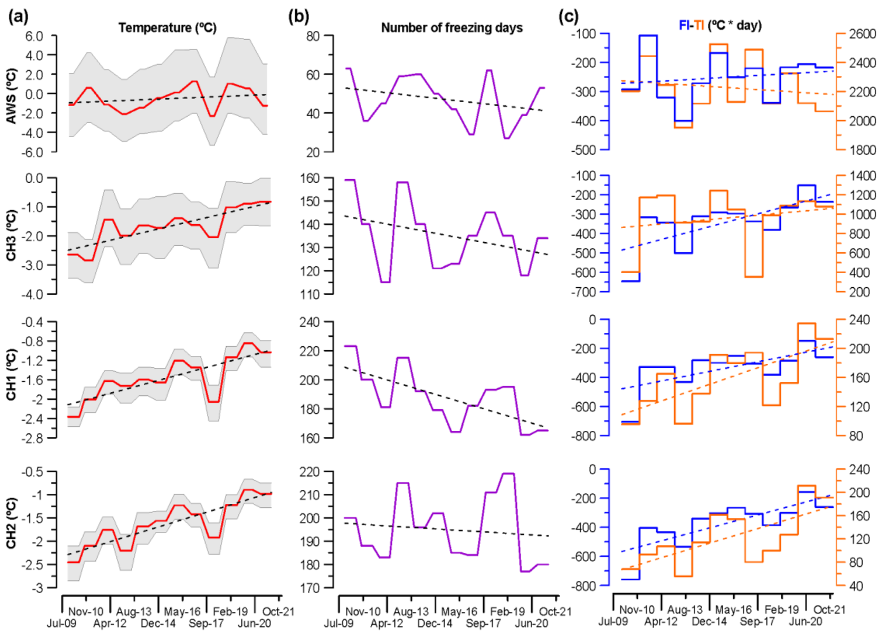

Figure 7: a) Variation of winter mean temperature at Armeña Weather Station (AWS), and mean cave temperatures for each sensor during the open phase. b) Variation of the number of freezing days outside and inside of A294. c) Freezing and Thaw indexes (°C hours per year) at AWS and in A294 during the study period.

In terms of precipitation (Fig. 8), the Armeña cirque received considerable monthly rainfall of more than 200 mm in October 2012, June 2015, November 2016, May 2017, November 2019, April and October 2020, and September 2021. The rainiest

https://doi.org/10.5194/egusphere-2025-8
Preprint. Discussion started: 3 March 2025

periods, spanning from April to November (mainly liquid precipitation), occurred between 2013 and 2016 (Fig. 8a). 2015 was particularly remarkable with 989 mm of rainfall. Similarly high values occurred between 2019 and 2021, with a remarkable 1312 mm of cumulated rainfall in 2020. These periods are also correlated with a higher frequency of rainy days. 2014 recorded the highest number of rain events (126), of which 46 and 51 events occurred during summer and fall, respectively. Years 2013 and 2020 were also notable, with 122 (46 in summer; 39 in fall) and 123 (39 in spring; 39 in summer; 44 in fall) rainfall events, respectively. Extreme rainfall events (exceeding 80 mm) occurred at the end of October and early November in 2011 (102 and 91 mm), November 2016 (83 and 86 mm), and July and October 2017 (131 and 111 mm). The amount of rainfall and the number of rainy days increased during the monitoring period (Fig. 8a). The cumulative snow accumulation (Góriz meteorological station) was close to or exceeded 2 m in the winters of 2008-2009, 2009-2010, 2012-2013, 2014-2015, 2016-2017, and 2017-2018. In contrast, the winter of 2011-2012 stands out with the lowest snow accumulation, reaching a maximum of 80 cm.

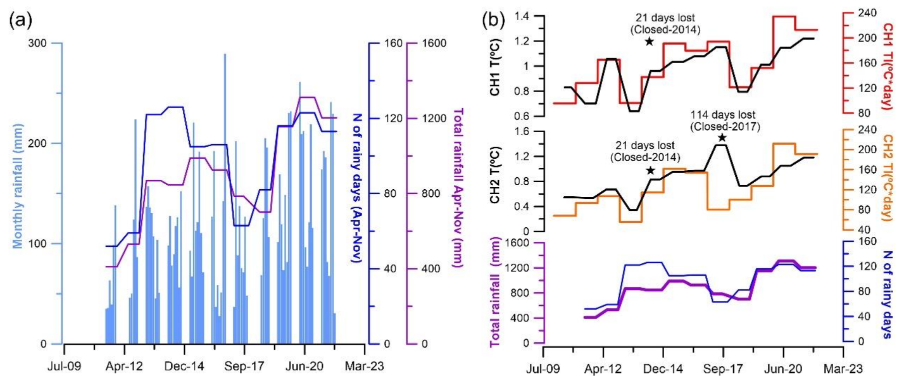

Figure 8: a) Monthly rainfall (April-November, light blue vertical bars) and the number of rainy days (dark blue line) and total rainfall (purple line). b) Mean cave air temperature and Thaw Index (TI) during the closed phase at sensors CH1 and CH2 compared to the number of rainy days (dark blue line) and total rainfall (purple line).

https://doi.org/10.5194/egusphere-2025-8
Preprint. Discussion started: 3 March 2025

4.3 Cave dynamics and external climate connections

The cave sensors recorded pronounced seasonal fluctuations during the winter. CH3 and CH2 sensors exhibit the highest mean correlations (r) (n=12, 12 years) between the outside winter mean air temperature and the cave air temperature during the open phase, with values of 0.78 ($p<0.001$) and 0.72 ($p<0.001$), respectively. CH1 shows a slightly lower correlation of 0.69 ($p<0.001$). The highest correlation was observed during the coldest winters, such as in 2017-2018 (CH1: 0.80, $p<0.001$) and 2012-2013 (CH2: 0.86, $p<0.001$). CH3 often shows high correlations, for example in the years 2019-2020 and in the winters between 2011 and 2013 (0.88, $p<0.001$; 0.86, $p<0.001$; and 0.83, $p<0.001$), indicating a stronger influence of the outside temperature in those periods. Conversely, during the warmest winter (2016-2017), the cave sensors recorded the lowest correlations (CH1: 0.46, $p<0.001$; CH2: 0.46, $p<0.001$; CH3: 0.50, $p<0.001$). The influence of winter temperature during the open phase causes a thermal impact in the subsequent closed phase, particularly at the deepest sensor, CH2 (Fig. S4).

Rainfall exerts a considerable impact on the cave air temperature, leading to short temperature rises (around +1.2 °C) during the closed phase (Fig. 8b). The trends observed in cave temperature and TI at CH1 and CH2 during the closed phase show a strong similarity with the total rainfall recorded at the AWS (Fig. 8b). The absence of distinct pattern at CH3 (not shown) may relate to its location close to the upper cave entrance. The Thaw Index, the temperature during the closed phases and the total rainfall (with the exception of the 2014 and 2017 periods, for which no data is available) exhibit strong correlations, but are not statistically significant (rainfall vs. TI-CH1: 0.71, $p=0.03$; rainfall vs. TI-CH2: 0.83, $p=0.006$; rainfall vs. T-CH1: 0.65, $p=0.05$; rainfall vs. TI-CH2: 0.82, $p=0.0082$). When removing the closed phase (due to the exceptionally cold winter of 2013), all correlations increase, and one (TI-CH2) becomes statistically significant (rainfall vs. TI-CH1: 0.76, $p=0.03$; rainfall vs. TI-CH2: 0.90, $p=0.002$; rainfall vs. T-CH1: 0.69, $p=0.06$; rainfall vs. T-CH2: 0.88, $p=0.007$). The data indicates that extreme rainfall events (exceeding 80 mm) trigger a more substantial temperature increase compared to what is typically observed during the

https://doi.org/10.5194/egusphere-2025-8
Preprint. Discussion started: 3 March 2025

closed phase. This is particularly evident in the data from October and November 2011 (Fig. S5).

4.4 Ice Loss

Throughout the 12-year monitoring period, substantial changes in the ice body have become apparent (Fig. 9)). These observations are supported by photographic evidence, field measurements, and comparisons with cave surveys dating back to the late 1970s. The most significant changes are related to the lateral retreat of the ice body from the northern (points 1 and 2) and the eastern (point 3) cave walls (Fig.3).

A comparison of cave surveys (horizontal retreat) conducted on the North wall (point 1) from 1978 to 2012 indicates a mean ice retreat of ~480 cm since 1978 (ranging between approximately 220 cm to 800 cm, n=9), equalling an annual loss of about 14.3 cm. However, the most significant change was observed during the 2019 survey when sections of the ice had completely vanished between the North and South walls (Figs. 3c and 10 a, b, c, d, e, f). Between 2012 and 2019, the mean ice loss was approximately 1370 cm (ranging between ~1240 cm to 2100 cm, n=8), translating to an average loss of approximately 196 cm a^{-1}. The Rock corner (point 2) remained almost stable between 2008 and 2011 (Fig. 10a, b). Measurements taken by a laser distance meter between 2011 and 2023 (Fig. 10 c, d, e) revealed an ice loss of ~435 cm (retreat rate of ~62 cm a^{-1}, n=1, between 2011and 2018) and ~610 cm (retreat rate of ~43 cm a^{-1}, n=1, between 2018 and 2022, Fig. 10e, f). In 2023, the total ice loss was ~753 cm (rate ~143 cm a^{-1}, n=3, between 2022 and 2023).

Concerning the East wall (point 3), the ice body was in contact with the wall until 2014 (Fig. 9a, b, c). Observations of seasonal ice stalagmites indicate that IS1 formed on the boulders at the cave floor from 2014 (Fig. 9c, July 2014), underlining the retreat of part of the ice deposit from the eastern wall. Nevertheless, IS2 remained over the ice deposit (Fig. 9c).

https://doi.org/10.5194/egusphere-2025-8
Preprint. Discussion started: 3 March 2025

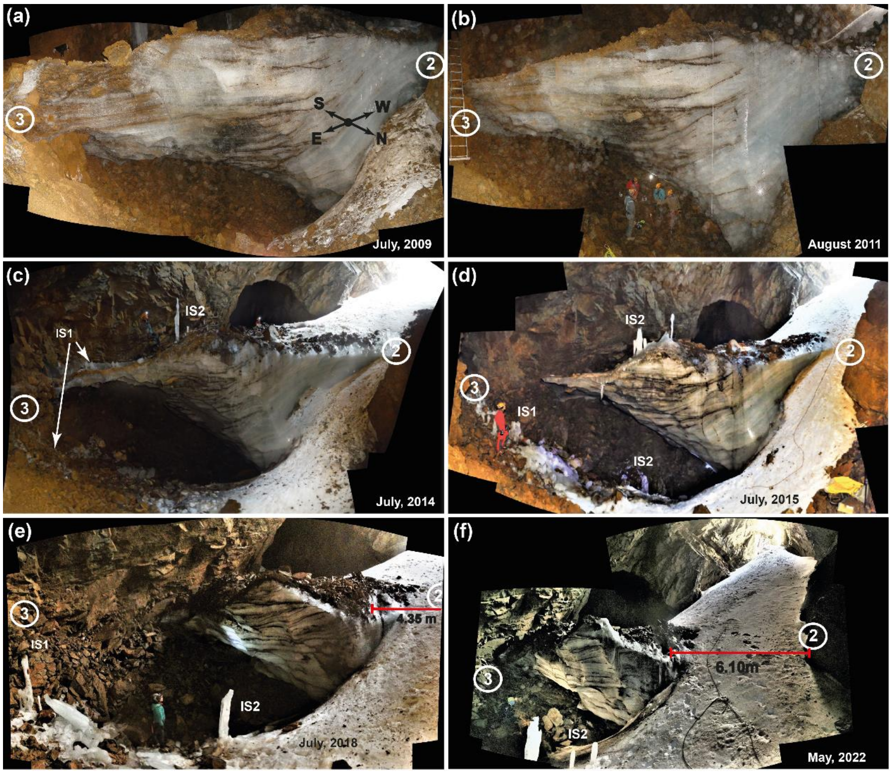

Figure 9: Panorama photos of the A294 ice body between 2009 and 2022 (a, b, c, d, e, f). The ice body was in contact with the East wall (3) between 1978, such as the cave survey indicates, and 2014 when the ice body retreated. The retreat of ice body from the North wall (1) and the Rock corner (2) is also documented by photos showing the width of the snow ramp. Seasonal ice stalagmites (IS1 and 2).

Between 2014 and 2015, the ice retreated approximately 410 cm (n=2) due to the collapse of the overhanging sector (Fig. 9c, d). In 2018, IS2 formed on the boulders, as well as in 2022 (see Fig. 9e, f). The cave survey in 2019 indicates a mean ice loss of about 960 cm (retreat rate of ~166 cm a^{-1} n=3, 2015-2019). This rate is similar to the one calculated for the North wall (196 cm a^{-1}; 2012-2019). In 2023, the ice front was 1300 cm (n=3) from the East wall (~100 cm a^{-1}, 2019-2023). Lastly, vertical changes in the ice deposit based on stratigraphic comparisons (Sancho et al., 2018; Leunda et al., 2019), Fig. S3) reveal an ice retreat of about 60 cm between 2011 and 2015, which corresponds to approximately ~15 cm a^{-1}. The evolution of the

https://doi.org/10.5194/egusphere-2025-8
Preprint. Discussion started: 3 March 2025

overhanging shape was difficult to assess due to the continuous change in the cave floor morphology caused by rockfalls from the upper part of the deposit due as a result of ice retreat. A continuous decrease was observed from 2009 until 2015, when the overhanging ice collapsed. The presence of a warm airflow associated with a deeper karst system (e.g. Bertozzi et al., 2019), which would explain the overhanging shape, is ruled out as the CH2 sensor shows the coldest temperatures. Probably, this shape is related to ice sublimation associated with local air circulation, as suggested by the presence of scallops.

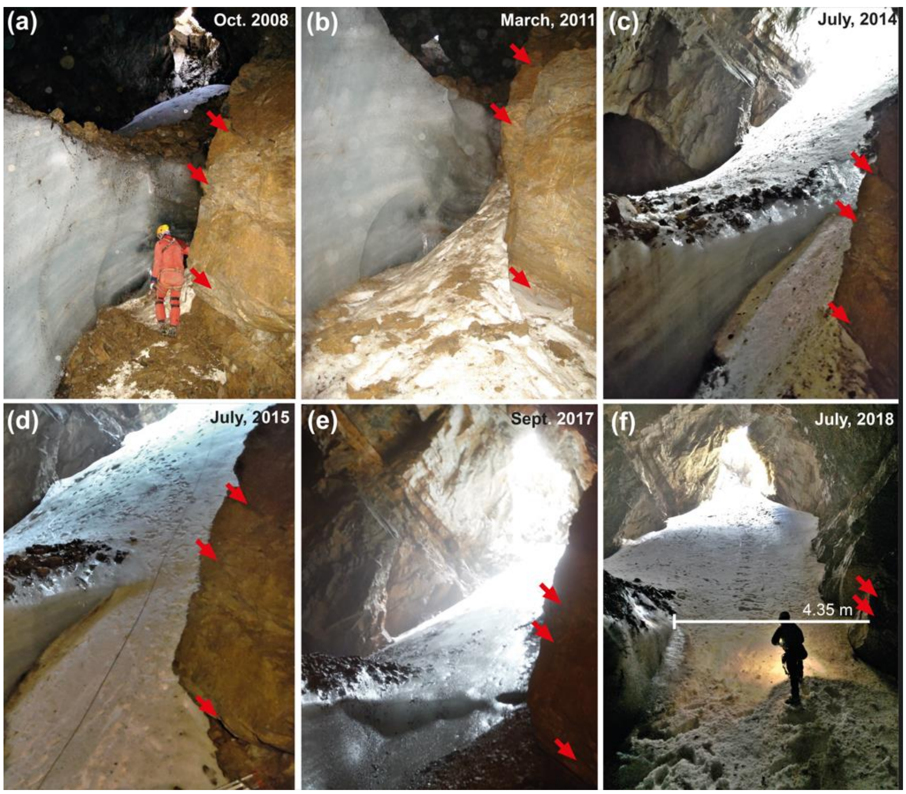

Figure 10: Changes and evolution of point 2 (Rock corner) between 2008 and 2018. Red arrows show fix points.

5. Discussion

5. 1 Climate control on the melting rate

https://doi.org/10.5194/egusphere-2025-8
Preprint. Discussion started: 3 March 2025

During winter, there is a strong correlation between cave air and outside air temperature, indicating the ingress of cold, dense air during open phases, leading to cave refrigeration. This open ventilation pattern is commonly observed in ice caves (e.g. Luetscher et al., 2008; Perşoiu et al., 2021; Wind et al., 2022). The correlation diminishes during warmer winters, such as in 2016-2017, implying reduced cave refrigeration. Additionally, the temperature recorded in A294 during open phases influences also the thermal regime during subsequent closed phases, similar to observations in other sag-type cave (Wind et al., 2022). Moreover, the positive temperatures recorded during closed phases indicate heat transfer from dripping points to the cave atmosphere consistent with the rainfall record, as evidenced by temperature increases following extreme rainfall events. Notably, during the exceptionally cold winter of 2012-2013, the cave was well refrigerated, resulting in low temperatures during the subsequent closed phase, while the impact of rainfall on cave temperature was almost negligible (Fig. 3b). This reduced influence of rainfall during the closed phase when the cave is well-refrigerated suggests that the heat transported by seepage water is exchanged primarily in the host rock and does not reach the cave atmosphere. Similarly, during snow-rich winters the cave temperature during the closed phase may be impacted by the thermal inertia of snow accumulation in the cave.

The temperature increase observed during the open phases in the cave (between ~1.07 and 1.56 ºC) exceeded the increase of winter temperature (~0.86 ºC). Inside the cave, 2009-2010 marked the coldest winter of the monitoring period. In contrast, the winter of 2009-2010 was less cold and only 0.2 ºC below the reference period 1971-2000, unlike 2011-2012 (third coldest winter of the 21st century) and 2017-2018 (seventh coldest winter since the beginning of 21st century in Spain) (AEMET, 2010, 2012, 2018). The analysis of the AWS climate data reveals that there were 41 days with temperatures below 4 °C during December, January, and February (D, J, F; the coldest months of the open phase). This is the highest number of days with temperatures below -4 °C in the entire external temperature record. The predominance of cold days during the winter of 2009–2010 likely contributed to the lowest mean temperature in the cave.

https://doi.org/10.5194/egusphere-2025-8
Preprint. Discussion started: 3 March 2025

The calculated ice retreat is similar for the North wall (point 1) and the East wall (point 3). However, the retreat is lower for the Rock Corner (point 2) and along the vertical axis. These differences are due to the fact that the Rock Corner and the basal part of the ice ramp are supplied each year by snow (and previously by the formation of seasonal congelation ice). As a result, snow and ice must melt first every year before the old ice layers thaw. Our observations suggest that the continuous retreat of the ice body over the last decade is related to i) the steady increase in winter temperature, which has reduced the heat exchange (i.e. cooling) during the open phase, and ii) the increase in rainfall (amount and number of days) between April and November. The freezing capacity of the snow and water entering the cave seems to have diminished, promoting continuous melting.

5.2 Unprecedented ice melt since 6100 years ago

Following the Holocene Thermal Maximum (HTM, Fig. 11), during which the global mean surface temperature was 0.7 °C warmer than the median of the 19^{th} century (Kaufman et al., 2020), the onset of the Neoglacial period (~6000-5000 years ago) was accompanied by large glacier advances (García-Ruiz et al., 2020). Those advances were associated with cooling periods in the North Atlantic region leading to a progressive temperature drop (Wanner et al., 2011; Bohleber, 2019). In the nearby Basa de la Mora lake (BSM, 3.6 km NW of the cave), the beginning of the Neoglacial is characterized by a drop in July temperatures of ~1.5 °C based on chironomids (Tarrats et al., 2018) (Fig. 11a).

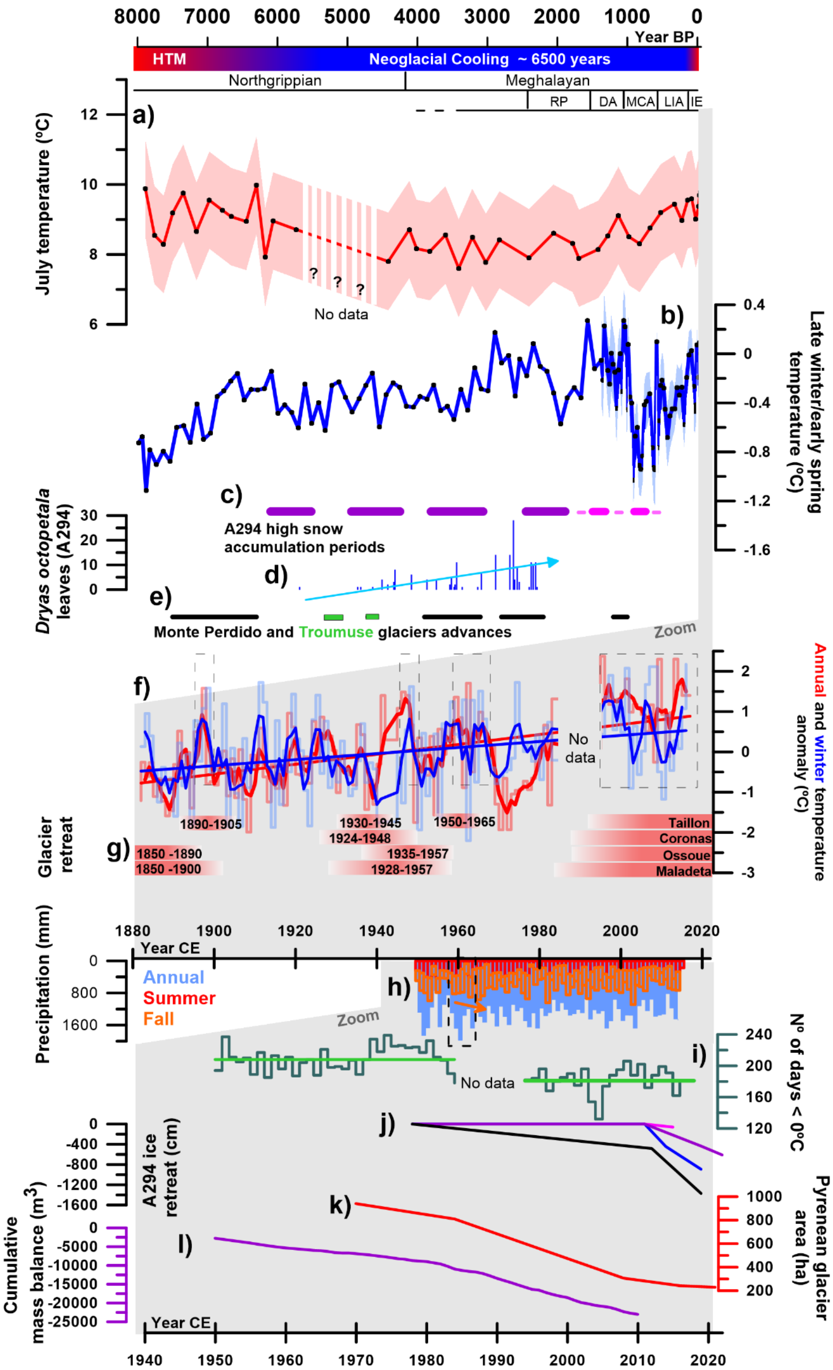
Year BP
HTM
Neoglacial Cooling ~ 6500 years
Northgrippian
Meghalayan
RP
DA
MCA
LIA
IE
a)
July temperature (ºC)
No data
b)
Late winter/early spring temperature (ºC)
c)
A294 high snow accumulation periods
d)
Dryas octopetala leaves (A294)
e)
Monte Perdido and Troumuse glaciers advances
Zoom
f)
No data
Annual and winter temperature anomaly (ºC)
g)
Glacier retreat
1890-1905
1930-1945
1924-1948
1950-1965
1850 -1890
1850 -1900
1935-1957
1928-1957
Taillon
Coronas
Ossoue
Maladeta
Year CE
Precipitation (mm)
Annual
Summer
Fall
h)
Zoom
i)
No data
Nº of days < 0ºC
j)
A294 ice retreat (cm)
k)
Pyrenean glacier area (ha)
l)
Cumulative mass balance (m3)
Year CE

https://doi.org/10.5194/egusphere-2025-8
Preprint. Discussion started: 3 March 2025

Figure 11: a) July temperatures reconstructed from chironomids (Tarrats et al., 2018). b) Winter-spring temperatures reconstructed from chrysophyte cysts in Lake Redón (Pla and Catalan, 2005). c) High snow accumulation in A294: purple from Sancho et al. (2018), pink from this study. d) Number of *Dryas octopetala* macrofossils in the A294 ice body (Leunda et al., 2019). e) Advances of Monte Perdido and Troumouse glaciers (Gellatly et al., 1992; García-Ruiz et al., 2014, 2020). f) Mean annual temperature (red) and winter anomaly (blue) from Pic du Midi de Bigorre (period 1882-2008) weather station (2860 m a.s.l., Bücher and Dessens, 1991; Dessens and Bücher, 1995). g) Glacier retreat in the Central Pyrenees (Marti et al., 2015). h) Annual precipitation (blue), summer (red), and fall (orange) from a Torla weather station located 39 km NW of A294 at 1053 m a.s.l. i) Evolution of freezing days calculated from the Pic du Midi de Bigorre weather station. j) Ice loss (cm) in A294: lines show vertical loss (pink), Rock Corner (blue, point 2), East wall (purple, point 3), and North wall (black, point 1). k) Changes in Pyrenean glacier area (ha) (Rico et al., 2017; Vidaller et al., 2021). l) Global cave ice loss - cumulative mass balance (m³) of ice caves (Kern and Perşoiu, 2013).

This temperature drop, and the relative stable winter-spring temperatures reconstructed from chrysophyte cysts at lake Redón (Pla and Catalan, 2005) during most of the Neoglacial (Fig. 11b), the cessation of tufa formed during part of the HTM (from 8700±134 to 6637±78 year cal. BP) in the San Bizién creek in the Cotiella massif (Belmonte, 2014), are coherent with the beginning of snow and ice accumulation in the A294 approximately 6100 years ago (Sancho et al., 2018) (Fig. 11c). In response to the relatively cold conditions following the HTM, an increase in the number of *Dryas octopetala* leaves found (Fig. 11d) within the ice body in A294 indicates the establishment of alpine meadows (dominated by *D. octopetala*), and a subsequent decline of the tree line ecotone (Leunda et al., 2019). Glaciers also responded to this cooling by advancing in the nearby cirques of Monte Perdido (García-Ruiz et al., 2020; Fig. 1c) (6900±800 ^{36}Cl yr BP) and Troumuse (Gellatly et al., 1992) (6190-5735, 5905-5485 years cal. BP) (28 km to the Northwest) (Fig. 11e). During the Neoglacial, phases of high ice accumulation occurred at 6100-5515, 4945-

https://doi.org/10.5194/egusphere-2025-8
Preprint. Discussion started: 3 March 2025

4250, 3810-3155, and 2450–1890 cal. BP in A294 (Fig. 11c), while other advances occurred in the Monte Perdido glacier at ~3500±400, ~2500±300, and ~1100±100 yr BP, and during the Little Ice Age (LIA) (García-Ruiz et al., 2014). Sancho et al. (2018) and Leunda et al. (2019) suggested that the ice accumulation in the A294 ice cave ended in the Roman Period (RP), a well-known warm period in the Iberian Peninsula and in the Central Pyrenees (Morellón et al., 2009; Martín-Puertas et al., 2010; Cisneros et al., 2016; Margaritelli et al., 2020; Bartolomé et al., 2024).

Our new radiocarbon dates, however, indicate that the ice accumulation continued during the Dark Ages (DA) (1409±99 cal. BP), a cold period in the Pyrenees, (Bartolomé et al., 2024), while the final ice accumulation took place 821±85 years ago corresponding to the end of the Medieval Climate Anomaly (MCA). During the MCA, summer temperature reconstructions based on Pyrenean tree-rings show similar warm temperatures as those in the 20th Century (Büntgen et al., 2017), while the Monte Perdido glacier suffered from important melting episodes (Moreno et al., 2021). The age (821±85 years cal. BP) of the current top of the deposit, located ~15 m above the main ice body, suggests the cave could have been completely filled with snow and ice during the LIA. The lack of ice from the Little Ice Age (LIA), however, suggests two potential scenarios (Sancho et al., 2018): firstly, that ice may have formed during the LIA and then subsequently melted away. Alternatively, it is plausible that the cave entrance was blocked due to the intensified and recurrent snowfall characteristic of the LIA, thereby preventing snow from entering the cave.

The current thick accumulation of debris on top the ice body at the foot of the ramp may have resulted from ice melt since the end of the LIA. This is likely given the increasing temperatures that affected the ice body near the entrance, while the morphology of the ice ramp has been preserved by seasonal snow accumulation at the cave entrance. We suggest that the top of the ice body has been affected by a negative mass balance since the LIA, while the oldest layers of the deposit have only been affected more recently, as the oldest cave survey shows.

https://doi.org/10.5194/egusphere-2025-8
Preprint. Discussion started: 3 March 2025

In the A294 ice cave, data about the past ice mass balance can be obtained from the analysis of the ice stratigraphy. Steep and vertical surfaces similar to those resulting from the current melting are absent in the ice succession. If a similar melting phase had occurred in the past, the ice stratigraphy would show truncated strata and high-angle unconformities due to accommodation following aggradation phases. The ice stratigraphy and the local climate reconstructions (Sancho et al., 2018; Tarrats et al., 2018; Leunda et al., 2019; García-Ruiz et al., 2020) therefore suggest that the ice melt in the last 6100 years was never as significant as it is today. This interpretation is consistent with the ongoing retreat of the Monte Perdido glacier and others Pyrenean glaciers (e.g. López-Moreno et al., 2016, 2019; Vidaller et al., 2021, 2023), which suggests that the current warming in the Pyrenees is the fastest and the most intense of the last 2000 years (Moreno et al., 2021), while current global temperatures are the highest in the last 6500 years (Kaufman et al., 2020).

5.3 The beginning of the end

The onset of the current ice retreat in A294 is difficult to determine. The 1978 cave survey indicates that the ice body covered almost the entire cave perimeter, except for a small pit hole and rimaye. The temperature (annual and winter) anomaly record of the Pyrenees (Midi de Bigorre station, at 2862 m a.s.l., Fig. 11f) shows a continuous temperature increase since 1880 (beginning of the record) with warm periods between 1890 and 1900, during the 1940's, around 1955-1970, and in recent decades (dashes rectangles, Fig. 11f). The Central Pyrenean glaciers (Marti et al., 2015 and references therein) show three main retreat phases since the end of the LIA (~1850 -1900; ~1924 -1965; 1980 – today, Fig. 11g), with slightly heterogeneous responses, which could be attributed to the generally larger influence of the local topography on smaller glaciers (Vidaller et al., 2021).

On the other hand, the annual regional precipitation anomaly series (1910-2013, 2535 m a.s.l.) for the Central Pyrenees shows a high inter-annual variability and a slightly negative and not significant trend of -0.6 °C decade^{-1} (Pérez-Zanón et al., 2017). Unfortunately, the high-altitude meteorological stations in the nearby areas

https://doi.org/10.5194/egusphere-2025-8
Preprint. Discussion started: 3 March 2025

only started monitoring in 1950. Therefore, to evaluate rainy periods, we have used the nearest long-term precipitation series (Fig. 11h) located 39 km NW of the A294 at 1053 m a.s.l. (Torla station). A relatively warm period associated with an increase in summer rainfall led to a glacier retreat in the 1960s and an increase in fall precipitation until the year 1970 (dashed rectangle, Fig. 11h). This precipitation increase in fall was also registered at a regional scale (Pérez-Zanón et al., 2017). These observations, together with the 1978 cave survey, suggest that the observed ice retreat could have started as early as the 1960s.

Between 1978 and 2012, the ice body in the A294 ice cave retreated, particularly at the North wall. After 1980 an important drop in freezing days is observed (Fig. 11i), as a consequence of a general increase in winter temperature. This situation led to a long-term snow decline below 2000 m a.s.l. (López-Moreno et al., 2020), which, together with an increase in rainfall during the warm season, favoured ice melt in the cave. The clear increase in melting rate between 2014 and 2019 (Fig. 11j) coincides with an important ice loss of up to 15 m (~6.1 m on average) on the Monte Perdido glacier between 2011 and 2020 (Vidaller et al., 2021). The continuous loss of ice in A294 was also coincided with an important phase of glacier retreat in the Pyrenees (Fig. 11k) (Rico et al., 2017; Vidaller et al., 2021). On a global scale, many ice caves are experiencing an important reduction in their ice volume (Fig. 11l) in response to te current climate warming (e.g. Luetscher et al., 2005; Kern and Perşoiu, 2013; Serrano et al., 2018; Colucci and Guglielmin, 2019; Perşoiu et al., 2021). However, the ice loss in A294 contrasts with other Pyrenean areas located in discontinuous mountain permafrost where the cave ice bodies are still protected from the current warming (Bartolomé et al., 2023). The A294 ice cave is a clear example of the current loss of paleoclimate information. Fortunately, some of this valuable information was recovered in time (Sancho et al., 2018; Leunda et al., 2019; Ruiz-Blas et al., 2023). Thus, we encourage the scientific community to study the valuable information stored in cave ice before this paleoenvironmental archive is lost forever.

https://doi.org/10.5194/egusphere-2025-8
Preprint. Discussion started: 3 March 2025

Conclusions

The investigation of A294 ice cave, based on environmental monitoring and ice melt tracking, as well as the stratigraphy and chronology of the deposit and its comparison with other paleoclimate records in the area, provides relevant information on the current ice melting and associated mechanisms.

Cave air temperature has risen by approximately 1.07 to 1.56 °C from 2009 to 2021. This warming is attributed to i) an increase in winter temperature, affecting the cave temperature during the open phase of refrigeration, and ii) an increase in rainfall during late spring, summer, and early fall, which transports heat through dripping points during the closed phase.

The increase in cave temperature and rainfall, along with reduced snowfall, has led to a continuous retreat of the ice body. The elevated cave temperatures have resulted in a diminished capacity to freeze water and snow entering the cave. In cave areas affected by seasonal snow and ice formation retreat rates are lower (~15-43 cm a^{-1}), whereas in other sectors the rates reached 196 cm a^{-1}.

The new samples obtained in 2022 after the complete disappearance of the snow ramp indicate that ice accumulation was maintained during the Dark Ages and part of the Medieval Climate Anomaly. The chronology, the ice stratigraphy, the ice retreat under current climate conditions, the paleoclimate record in the area, as well as older cave surveys indicate that the current ice melt is the most intense in the last 6100 years, when the deposit began to form.

At current and projected future rates of climate change, it is very likely that the current melting will continue or even increase and that the ice deposit in A294 will vanish within the next decade, although a portion of the ice may remain partially preserved beneath the seasonal snow accumulation zone.

https://doi.org/10.5194/egusphere-2025-8
Preprint. Discussion started: 3 March 2025

Data availability

Data are available from the authors upon request.

Supplement

Author contributions

CSa, ÁB, MB conceived the idea and designed the strategy. MB, ÁB, MLe performed fieldwork, sensor download and maintenance, and a cave survey in 2019. MB conducted data analyses and designed the figures. JIL-M provided quantile temperature series and reviewed climatic data. CSa and AM obtained the funding. MB wrote the draft manuscript including all inputs, suggestions and revisions from AM, ÁB, MLe, MLu, CSp, JIL-M, BO-U, JL-M.

Competing interests

The contact author has declared that none of the authors has any competing interests.

Acknowledgements

In memory of Carlos Sancho. This paper is a tribute to our dear friend and colleague, Dr. Carlos Sancho (Fig. 12), who passed away too soon. We extend our sincere gratitude to Jean Claude Gayet, Ramón Queraltó, Carles Pons (Asociación Cientifico-Espeleológica Cotiella, ACEC), Alexandra Bozonet, Reyes Giménez, David Serrano and Mario Bielsa for setting up the Armeña weather station and for their help during fieldwork. We thank the AEMET (Agencia Estatal de Meteorología) foe for providing the data from the Góriz station.

https://doi.org/10.5194/egusphere-2025-8
Preprint. Discussion started: 3 March 2025

Figure 12: Dr. Carlos Sancho during fieldwork in a cave.

Financial support

This work was supported by the Spanish Government and the European Regional Development Funds (OPERA, SPYRIT, PYCACHU, ORCHESTRA CGL2009-10455/BTE, CTM2013-48639-C2-1-R, and CGL2016-77479-R).

References

Agencia Estatal de Meteorología (AEMET). 2010. Resumen estacional climatológico. Invierno 2009-2010. Ministerio de Medio Ambiente y Medio Rural y Marino. Gobierno de España. 6 pp. https://www.aemet.es/documentos/es/elclima/datos_climat/resumenes_climat/estacionales/2010/Est_invierno_092010.pdf

Agencia Estatal de Meteorología (AEMET). 2012. Resumen estacional climatológico. Invierno 2011-2012. Ministerio de Agricultura, Alimentación y Medio Ambiente. 7 pp https://repositorio.aemet.es/bitstream/20.500.11765/1220/1/Est_invierno_11_12.pdf

Agencia Estatal de Meteorología (AEMET). 2018. Resumen estacional climatológico. Invierno 2017-2018. Ministerio de Agricultura y Pesca, Alimentación y Medio Ambiente. 7 pp https://www.aemet.es/documentos/es/serviciosclimaticos/vigilancia_clima/resumenes_climat/estacionales/2018/Est_invierno_17_18.pdf

Bartolomé, M., Cazenave, G., Luetscher, M., Spötl, C., Gázquez, F., Belmonte, Á., Turchyn, A.V., López-Moreno, J.I., Moreno, A., 2023. Mountain permafrost in the Central Pyrenees: insights from the Devaux ice cave. The Cryosphere 17, 477–497. https://doi.org/10.5194/tc-17-477-2023

Bartolomé, M., Moreno, A., Sancho, C., Cacho, I., Stoll, H., Haghipour, N., Belmonte, Á., Spötl, C., Hellstrom, J., Edwards, R.L., Cheng, H., 2024. Reconstructing hydroclimate changes over the past 2500 years using speleothems from Pyrenean caves (NE Spain). Climate of the Past 20, 467–494. https://doi.org/10.5194/cp-20-467-2024

Beguería, S., Tomas-Burguera, M., Serrano-Notivoli, R., Peña-Angulo, D., Vicente-Serrano, S.M., González-Hidalgo, J.-C., 2019. Gap filling of monthly temperature data and its effect on

https://doi.org/10.5194/egusphere-2025-8
Preprint. Discussion started: 3 March 2025

climatic variability and trends. Journal of Climate 32, 7797–7821. https://doi.org/10.1175/JCLI-D-19-0244.1

Belmonte, Ánchel, 2014. Geomorfología del macizo de Cotiella (Pirineo oscense): cartografía, evolución paleoambiental y dinámica actual. Tesis Doctoral. Universidad de Zaragoza.

Belmonte-Ribas, Á., Sancho, C., Moreno, A., Lopez-Martinez, J., Bartolome, M., 2014. Present-day environmental dynamics in ice cave a294, central pyrenees, spain. Geografia Fisica e Dinamica Quaternaria 37, 131–140. https://doi.org/10.4461/GFDQ.2014.37.12

Bertozzi, B., Pulvirenti, B., Colucci, R.R., Di Sabatino, S., 2019. On the interactions between airflow and ice melting in ice caves: A novel methodology based on computational fluid dynamics modeling. Science of The Total Environment 669, 322–332. https://doi.org/10.1016/j.scitotenv.2019.03.074

Biskaborn, B.K., Smith, S.L., Noetzli, J., Matthes, H., Vieira, G., Streletskiy, D.A., Schoeneich, P., Romanovsky, V.E., Lewkowicz, A.G., Abramov, A., Allard, M., Boike, J., Cable, W.L., Christiansen, H.H., Delaloye, R., Diekmann, B., Drozdov, D., Etzelmüller, B., Grosse, G., Guglielmin, M., Ingeman-Nielsen, T., Isaksen, K., Ishikawa, M., Johansson, M., Johannsson, H., Joo, A., Kaverin, D., Kholodov, A., Konstantinov, P., Kröger, T., Lambiel, C., Lanckman, J.-P., Luo, D., Malkova, G., Meiklejohn, I., Moskalenko, N., Oliva, M., Phillips, M., Ramos, M., Sannel, A.B.K., Sergeev, D., Seybold, C., Skryabin, P., Vasiliev, A., Wu, Q., Yoshikawa, K., Zheleznyak, M., Lantuit, H., 2019. Permafrost is warming at a global scale. Nature Communications 10, 264. https://doi.org/10.1038/s41467-018-08240-4

Blaauw, M., 2010. Methods and code for 'classical' age-modelling of radiocarbon sequences. Quaternary Geochronology 5, 512–518. https://doi.org/10.1016/j.quageo.2010.01.002

Bohleber, P., 2019. Alpine ice cores as climate and environmental archives. Oxford Research Encyclopedia of Climate Science. https://doi.org/10.1093/acrefore/9780190228620.013.743

Bücher, A., Dessens, J., 1991. Secular trend of surface temperature at an elevated observatory in the Pyrenees. Journal of Climate 4, 859–868. https://doi.org/10.1175/1520-0442(1991)004<0859:STOSTA>2.0.CO;2

Büntgen, U., Krusic, P.J., Verstege, A., Sangüesa-Barreda, G., Wagner, S., Camarero, J.J., Ljungqvist, F.C., Zorita, E., Oppenheimer, C., Konter, O., Tegel, W., Gärtner, H., Cherubini, P., Reinig, F., Esper, J., 2017. New tree-ring evidence from the Pyrenees reveals Western Mediterranean climate variability since medieval times. Journal of Climate 30, 5295–5318. https://doi.org/10.1175/JCLI-D-16-0526.1

Cisneros, M., Cacho, I., Frigola, J., Canals, M., Masqué, P., Martrat, B., Casado, M., Grimalt, J.O., Pena, L.D., Margaritelli, G., Lirer, F., 2016. Sea surface temperature variability in the central-western Mediterranean Sea during the last 2700 years: a multi-proxy and multi-record approach. Clim. Past 12, 849–869. https://doi.org/10.5194/cp-12-849-2016

Colucci, R.R., Guglielmin, M., 2019. Climate change and rapid ice melt: Suggestions from abrupt permafrost degradation and ice melting in an alpine ice cave. Progress in Physical Geography: Earth and Environment 0309133319846056. https://doi.org/10.1177/0309133319846056

Dessens, J., Bücher, A., 1995. Changes in minimum and maximum temperatures at the Pic du Midi in relation with humidity and cloudiness, 1882–1984. Atmospheric Research, Minimax Workshop 37, 147–162. https://doi.org/10.1016/0169-8095(94)00075-O

Feurdean, A., Perşoiu, A., Pazdur, A., Onac, B.P., 2011. Evaluating the palaeoecological potential of pollen recovered from ice in caves: A case study from Scărişoara Ice Cave, Romania. Review of Palaeobotany and Palynology 165, 1–10. https://doi.org/10.1016/j.revpalbo.2011.01.007

García-Ruiz, J.M., Palacios, D., Andrés, N. de, Valero-Garcés, B.L., López-Moreno, J.I., Sanjuán, Y., 2014. Holocene and 'Little Ice Age' glacial activity in the Marboré Cirque, Monte

Perdido Massif, Central Spanish Pyrenees. The Holocene 24, 1439–1452. https://doi.org/10.1177/0959683614544053
García-Ruiz, J.M., Palacios, D., Andrés, N., López-Moreno, J.I., 2020. Neoglaciation in the Spanish Pyrenees: A multiproxy challenge. Journal of Mediterranean Geosciences 2, 21-26.
Gellatly, A.F., Grove, J.M., Switsur, V.R., 1992. Mid-Holocene glacial activity in the Pyrenees. The Holocene 2, 266–270. https://doi.org/10.1177/095968369200200309
González Trueba, J.J., Moreno, R.M., Martínez de Pisón, E., Serrano, E., 2008. `Little Ice Age' glaciation and current glaciers in the Iberian Peninsula. The Holocene 18, 551–568. https://doi.org/10.1177/0959683608089209
Hammer, O., Harper, D. A. T., Ryan, P. D., 2001. PAST: Paleontological statistics software package for education and data analysis. 4(1): 9pp. Palaeontologia Electronica 4 (1), 9.
Harris, S.A., 1981. Climatic Relationships of Permafrost Zones in Areas of Low Winter Snow-Cover. Arctic 34, 64–70.
Heeb, B., 2014. The next generation of the DistoX cave surveying instrument. CREG J., 88, 5-8.
IPCC, 2021: Climate Change 2021: The Physical Science Basis. Contribution of Working Group I to the Sixth Assessment Report of the Intergovernmental Panel on Climate Change [Masson-Delmotte, V., P. Zhai, A. Pirani, S.L. Connors, C. Péan, S. Berger, N. Caud, Y. Chen, L. Goldfarb, M.I. Gomis, M. Huang, K. Leitzell, E. Lonnoy, J.B.R. Matthews, T.K. Maycock, T. Waterfield, O. Yelekçi, R. Yu, and B. Zhou (eds.)]. Cambridge University Press, Cambridge, United Kingdom and New York, NY, USA, 2391 pp.
Kaufman, D., McKay, N., Routson, C., Erb, M., Dätwyler, C., Sommer, P.S., Heiri, O., Davis, B., 2020. Holocene global mean surface temperature, a multi-method reconstruction approach. Sci Data 7, 201. https://doi.org/10.1038/s41597-020-0530-7
Kern, Z., Perşoiu, A., 2013. Cave ice – the imminent loss of untapped mid-latitude cryospheric palaeoenvironmental archives. Quaternary Science Reviews 67, 1–7. https://doi.org/10.1016/j.quascirev.2013.01.008
Leunda, M., González-Sampériz, P., Gil-Romera, G., Bartolomé, M., Belmonte-Ribas, Á., Gómez-García, D., Kaltenrieder, P., Rubiales, J.M., Schwörer, C., Tinner, W., Morales-Molino, C., Sancho, C., 2019. Ice cave reveals environmental forcing of long-term Pyrenean tree line dynamics. Journal of Ecology 107, 814–828. https://doi.org/10.1111/1365-2745.13077
Lompar, M., Lalić, B., Dekić, L., Petrić, M., 2019. Filling gaps in hourly air temperature data using debiased ERA5 data. Atmosphere 10, 13. https://doi.org/10.3390/atmos10010013
López-Moreno, J.I., 2005. Recent variations of snowpack depth in the Central Spanish Pyrenees. Arctic, Antarctic, and Alpine Research 37, 253–260. https://doi.org/10.1657/1523-0430(2005)037[0253:RVOSDI]2.0.CO;2
López-Moreno, J.I., Alonso-González, E., Monserrat, O., Del Río, L.M., Otero, J., Lapazaran, J., Luzi, G., Dematteis, N., Serreta, A., Rico, I., Serrano-Cañadas, E., Bartolomé, M., Moreno, A., Buisan, S., Revuelto, J., 2019. Ground-based remote-sensing techniques for diagnosis of the current state and recent evolution of the Monte Perdido Glacier, Spanish Pyrenees. J. Glaciol. 65, 85–100. https://doi.org/10.1017/jog.2018.96
López-Moreno, J.I., García-Ruiz, J.M., Vicente-Serrano, S.M., Alonso-González, E., Revuelto-Benedí, J., Rico, I., Izagirre, E., Beguería-Portugués, S., 2020. Critical discussion of: "A farewell to glaciers: Ecosystem services loss in the Spanish Pyrenees." Journal of Environmental Management 275, 111247. https://doi.org/10.1016/j.jenvman.2020.111247
López-Moreno, J.I., Revuelto, J., Rico, I., Chueca-Cía, J., Julián, A., Serreta, A., Serrano, E., Vicente-Serrano, S.M., Azorin-Molina, C., Alonso-González, E., García-Ruiz, J.M., 2016. Thinning of the Monte Perdido Glacier in the Spanish Pyrenees since 1981. The Cryosphere 10, 681–694. https://doi.org/10.5194/tc-10-681-2016

Luetscher, M., Jeannin, P.-Y., Haeberli, W., 2005. Ice caves as an indicator of winter climate evolution: a case study from the Jura Mountains. The Holocene 15, 982–993. https://doi.org/10.1191/0959683605hl872ra

Luetscher, M., Lismonde, B., Jeannin, P.-Y., 2008. Heat exchanges in the heterothermic zone of a karst system: Monlesi cave, Swiss Jura Mountains. Journal of Geophysical Research: Earth Surface 113. https://doi.org/10.1029/2007JF000892

Margaritelli, G., Cacho, I., Català, A., Barra, M., Bellucci, L.G., Lubritto, C., Rettori, R., Lirer, F., 2020. Persistent warm Mediterranean surface waters during the Roman period. Sci Rep 10, 10431. https://doi.org/10.1038/s41598-020-67281-2

Marti, R., Gascoin, S., Houet, T., Ribière, O., Laffly, D., Condom, T., Monnier, S., Schmutz, M., Camerlynck, C., Tihay, J.P., Soubeyroux, J.M., René, P., 2015. Evolution of Ossoue Glacier (French Pyrenees) since the end of the Little Ice Age. The Cryosphere 9, 1773–1795. https://doi.org/10.5194/tc-9-1773-2015

Martín-Puertas, C., Jiménez-Espejo, F., Martínez-Ruiz, F., Nieto-Moreno, V., Rodrigo, M., Mata, M.P., Valero-Garcés, B.L., 2010. Late Holocene climate variability in the southwestern Mediterranean region: an integrated marine and terrestrial geochemical approach. Clim. Past 6, 807–816. https://doi.org/10.5194/cp-6-807-2010

Morellón, M., Valero-Garcés, B., Vegas-Vilarrúbia, T., González-Sampériz, P., Romero, Ó., Delgado-Huertas, A., Mata, P., Moreno, A., Rico, M., Corella, J.P., 2009. Lateglacial and Holocene palaeohydrology in the western Mediterranean region: The Lake Estanya record (NE Spain). Quaternary Science Reviews 28, 2582–2599.

Moreno, A., Bartolomé, M., López-Moreno, J.I., Pey, J., Corella, J.P., García-Orellana, J., Sancho, C., Leunda, M., Gil-Romera, G., González-Sampériz, P., Pérez-Mejías, C., Navarro, F., Otero-García, J., Lapazaran, J., Alonso-González, E., Cid, C., López-Martínez, J., Oliva-Urcia, B., Faria, S.H., Sierra, M.J., Millán, R., Querol, X., Alastuey, A., García-Ruíz, J.M., 2021. The case of a southern European glacier which survived Roman and medieval warm periods but is disappearing under recent warming. The Cryosphere 15, 1157–1172. https://doi.org/10.5194/tc-15-1157-2021

Observatorio Pirenaico de Cambio Global, 2018. Observatorio Pirenaico de Cambio Global: Executive summary report OPCC2: Climate change in the Pyrenees:impacts, vulnerability and adaptation.

Pérez-Zanón, N., Sigró, J., Ashcroft, L., 2017. Temperature and precipitation regional climate series over the central Pyrenees during 1910–2013. International Journal of Climatology 37, 1922–1937. https://doi.org/10.1002/joc.4823

Perşoiu, A., Buzjak, N., Onaca, A., Pennos, C., Sotiriadis, Y., Ionita, M., Zachariadis, S., Styllas, M., Kosutnik, J., Hegyi, A., Butorac, V., 2021. Record summer rains in 2019 led to massive loss of surface and cave ice in SE Europe. The Cryosphere 15, 2383–2399. https://doi.org/10.5194/tc-15-2383-2021

Perșoiu, A., Onac, B.P., Wynn, J.G., Blaauw, M., Ionita, M., Hansson, M., 2017. Holocene winter climate variability in Central and Eastern Europe. Scientific Reports 7, 1196. https://doi.org/10.1038/s41598-017-01397-w

Pla, S., Catalan, J., 2005. Chrysophyte cysts from lake sediments reveal the submillennial winter/spring climate variability in the northwestern Mediterranean region throughout the Holocene. Climate Dynamics 24, 263–278. https://doi.org/10.1007/s00382-004-0482-1

R Core Team, 2020. R: A Language and Environment for Statistical Computing. R Foundation for Statistical Computing, Vienna.

Racine, T.M.F., Reimer, P.J., Spötl, C., 2022a. Multi-centennial mass balance of perennial ice deposits in Alpine caves mirrors the evolution of glaciers during the Late Holocene. Sci Rep 12, 11374. https://doi.org/10.1038/s41598-022-15516-9

https://doi.org/10.5194/egusphere-2025-8
Preprint. Discussion started: 3 March 2025

Racine, T.M.F., Spötl, C., Reimer, P.J., Čarga, J., 2022b. Radiocarbon constraints on periods of positive cave ice mass balance during the last millennium, Julian Alps (NW Slovenia). Radiocarbon 64, 333-356. https://doi.org/10.1017/RDC.2022.26

Reimer, P.J., Austin, W.E.N., Bard, E., Bayliss, A., Blackwell, P.G., Ramsey, C.B., Butzin, M., Cheng, H., Edwards, R.L., Friedrich, M., Grootes, P.M., Guilderson, T.P., Hajdas, I., Heaton, T.J., Hogg, A.G., Hughen, K.A., Kromer, B., Manning, S.W., Muscheler, R., Palmer, J.G., Pearson, C., Plicht, J. van der, Reimer, R.W., Richards, D.A., Scott, E.M., Southon, J.R., Turney, C.S.M., Wacker, L., Adolphi, F., Büntgen, U., Capano, M., Fahrni, S.M., Fogtmann-Schulz, A., Friedrich, R., Köhler, P., Kudsk, S., Miyake, F., Olsen, J., Reinig, F., Sakamoto, M., Sookdeo, A., Talamo, S., 2020. The IntCal20 Northern Hemisphere radiocarbon age calibration curve (0–55 cal kBP). Radiocarbon 62, 725–757. https://doi.org/10.1017/RDC.2020.41

Rico, I., Izagirre, E., Serrano, E., López-Moreno, J.I., 2017. Superficie glaciar actual en los Pirineos: Una actualización para 2016. Pirineos 172, 029. https://doi.org/10.3989/Pirineos.2017.172004

Ruiz-Blas, F., Muñoz-Hisado, V., Garcia-Lopez, E., Moreno, A., Bartolomé, M., Leunda, M., Martinez-Alonso, E., Alcázar, A., Cid, C., 2023. The hidden microbial ecosystem in the perennial ice from a Pyrenean ice cave. Frontiers in Microbiology 14.

Sancho, C., Belmonte, Á., Bartolomé, M., Moreno, A., Leunda, M., López-Martínez, J., 2018. Middle-to-late Holocene palaeoenvironmental reconstruction from the A294 ice-cave record (Central Pyrenees, northern Spain). Earth and Planetary Science Letters 484, 135–144. https://doi.org/10.1016/j.epsl.2017.12.027

Serrano, E., Gómez-Lende, M., Belmonte, Á., Sancho, C., Sánchez-Benítez, J., Bartolomé, M., Leunda, M., Moreno, A., Hivert, B., 2018. Chapter 28 - Ice Caves in Spain, in: Perşoiu, A., Lauritzen, S.-E. (Eds.), Ice Caves. Elsevier, pp. 625–655. https://doi.org/10.1016/B978-0-12-811739-2.00028-0

Serrano-Notivoli, R., Tejedor, E., Sarricolea, P., Meseguer-Ruiz, O., de Luis, M., Saz, M.Á., Longares, L.A., Olcina, J., 2023. Unprecedented warmth: A look at Spain's exceptional summer of 2022. Atmospheric Research 293, 106931. https://doi.org/10.1016/j.atmosres.2023.106931

Stoffel, M., Luetscher, M., Bollschweiler, M., Schlatter, F., 2009. Evidence of NAO control on subsurface ice accumulation in a 1200 yr old cave-ice sequence, St. Livres ice cave, Switzerland. Quaternary Research 72, 16–26. https://doi.org/10.1016/j.yqres.2009.03.002

Tarrats, P., Heiri, O., Valero-Garcés, B., Cañedo-Argüelles, M., Prat, N., Rieradevall, M., González-Sampériz, P., 2018. Chironomid-inferred Holocene temperature reconstruction in Basa de la Mora Lake (Central Pyrenees). The Holocene 0959683618788662. https://doi.org/10.1177/0959683618788662

Tuhkanen, S., 1980. Climatic parameters and indices in plant geography. Acta phytogeographica Suecica 105.

Vidaller, I., Izagirre, E., del Rio, L.M., Alonso-González, E., Rojas-Heredia, F., Serrano, E., Moreno, A., López-Moreno, J.I., Revuelto, J., 2023. The Aneto glacier's (Central Pyrenees) evolution from 1981 to 2022: ice loss observed from historic aerial image photogrammetry and remote sensing techniques. The Cryosphere 17, 3177–3192. https://doi.org/10.5194/tc-17-3177-2023

Vidaller, I., Revuelto, J., Izagirre, E., Rojas-Heredia, F., Alonso-González, E., Gascoin, S., René, P., Berthier, E., Rico, I., Moreno, A., Serrano, E., Serreta, A., López-Moreno, J.I., 2021. Toward an ice-free mountain range: Demise of Pyrenean glaciers during 2011–2020. Geophysical Research Letters 48, e2021GL094339. https://doi.org/10.1029/2021GL094339

https://doi.org/10.5194/egusphere-2025-8
Preprint. Discussion started: 3 March 2025

Wanner, H., Solomina, O., Grosjean, M., Ritz, S.P., Jetel, M., 2011. Structure and origin of Holocene cold events. Quaternary Science Reviews 30, 3109–3123. https://doi.org/10.1016/j.quascirev.2011.07.010

Wind, M., Obleitner, F., Racine, T., Spötl, C., 2022. Multi-annual temperature evolution and implications for cave ice development in a sag-type ice cave in the Austrian Alps. The Cryosphere 16, 3163–3179. https://doi.org/10.5194/tc-16-3163-2022

Žák, K., Richter, D.K., Filippi, M., Živor, R., Deininger, M., Mangini, A., Scholz, D., 2012. Coarsely crystalline cryogenic cave carbonate – a new archive to estimate the Last Glacial minimum permafrost depth in Central Europe. Climate of the Past 8, 1821–1837. https://doi.org/10.5194/cp-8-1821-2012